Vol. A42 (1972) ACTA PHYSICA POLONICA No 2

INFLUENCE OF THE TRANSVERSAL MAGNETIC FIELD ON A UNIAXIAL FERROMAGNET WITH PLATE-LIKE DOMAIN STRUCTURE

By W. Wasilewski

Physics Department, College of Engineering, Kielce*

and W. J. Ziętek

Institute for Low Temperature and Structure Research, Polish Academy of Sciences, Wrocław**

(Received January 3, 1972)

The influence of a homogeneous external magnetic field on a uniaxial ferromagnet with plate-like Kittel-type domain structure is examined for the case when the field is perpendicular to the anisotropy axis and normal to the 180° Bloch walls. A hexagonal close-packed crystal lattice with nearest-neighbour exchange interactions is assumed, the anisotropy being described by pseudo-dipolar spin coupling. The Euler-Lagrange equation for the domain structure is solved under periodic boundary conditions, and analytic formulae for the field-dependence of the magnetization, susceptibility, wall thickness and wall energy are derived. Due to the neglect of the magnetostatic self-energy in the considerations, the numerical magnetization curve for Co is found to be in qualitative agreement with experimental data for fields up to 200 Oe only. In contrast to recent theoretical results obtained by other authors for single-domain uniaxial ferromagnets, the periodic domain structure is shown to cancel the field-induced second-order ferro-paramagnetic phase transition.

1. *Introduction*

The influence of a homogeneous external magnetic field on the plate-like Kittel-type domain structure [1] in uniaxial ferromagnets has first been examined in [2, 3] by employing the phenomenological macroscopic theory, and later in [4,5] by using the microscopic formalism proposed in [6] and elaborated in [7]. In the papers [2, 4], a field parallel to the anisotropy axis (longitudinal field) has been considered, while in [3, 5] the field has been assumed to be perpendicular to this axis (transversal field) but parallel

* Address: Zespół Fizyki, Kielecko-Radomska Wyższa Szkoła Inżynierska, Kielce, Aleja Tysiąclecia, Poland.

** Address: Instytut Niskich Temperatur i Badań Strukturalnych, Polska Akademia Nauk, Wrocław, Plac Katedralny 1, Poland.

to the 180° Bloch walls of the domain structure. A phenomenological uniaxial anisotropy has been assumed in [2, 3], whereas the analysis in [4, 5] was based on nearest--neighbour pseudo-dipolar spin interactions which lead automatically to uniaxial anisotropy in the respective crystal lattices [8–11]. The considerations in [4, 5] were confined to a simple hexagonal crystal lattice and have been extended in [12, 13] to a wide crystal class. Recently, the influence of the temperature on those magnetization processes has been studied qualitatively by using the molecular-field approach [14]. The displacement of Bloch walls under the influence of a longitudinal magnetic field has also been analysed theoretically in [15].

So far, the theory has not yet been extended to the case when the external field is perpendicular to the anisotropy axis but, at the same time, perpendicular to the Bloch walls. It is the aim of the present paper to study this case, by employing the formalism developed in [4–10] and assuming a close-packed hexagonal crystal lattice. This extension of the theory is the more desirable in view of the experimental results reported in [16, 17], where quite precise magnetization curves for single-crystalline Co have been obtained and shown to depend strongly on the type of domain structure. Moreover, in the case of the layerlike Goodenough-type domain structure the magnetization curves in [17] have also been found to depend on the orientation of the 180° Bloch walls with respect to the transversal magnetic field. On the other hand, theoretical investigations showed [18] that in uniaxial ferromagnets a perpendicular orientation of the Bloch walls in a transversal field is energetically most favourable.

There is one more reason for closer examining the influence of the transversal field on ferromagnets with domain structure, which resides in the newly discovered second-order ferro-paramagnetic phase transition that occurs in uniaxial single-domain ferromagnets in a transversal field. By now, this effect has been obtained by different methods in a number of papers [19–26]. We shall show that the plate-like domain structure with 180° walls cancels this phase transition if the field is perpendicular to the walls. This result may well explain why the existence of this particular phase transition is hard to prove experimentally [27].

2. *The energy of the system*

Following [4, 5], we start with the Hamiltonian

$$H = -\mu g \mathscr{H}^a \sum_i S_i^a - \tfrac{1}{2} \sum_{ij} P_{ij}^{ab} S_i^a S_j^b \tag{1}$$

where

$$P_{ij}^{ab} = \begin{cases} (J_{ij}+C_{ij})\delta^{ab} - 3C_{ij} r_{ij}^{-2} r_{ij}^a r_{ij}^b & \text{for nearest neighbours,} \\ 0 & \text{otherwise.} \end{cases} \tag{2}$$

Here μ denotes Bohr's magneton, g is Lande's splitting factor, $\mathscr{H}^a$ is the a-component of the external (homogeneous) magnetic field, S_i^a are spin operator components assigned to the lattice site i, r_{ij}^a are the components of the lattice vector from site i to site j, and $J_{ij} > 0$

and $C_{ij} < 0$ are respectively the Heisenberg exchange integral and the pseudo-dipolar coupling constant, both depending on the distance r_{ij} between the lattice sites i and j. To the tensor indices a, b (= 1, 2, 3) Einstein's summation rule is applied.

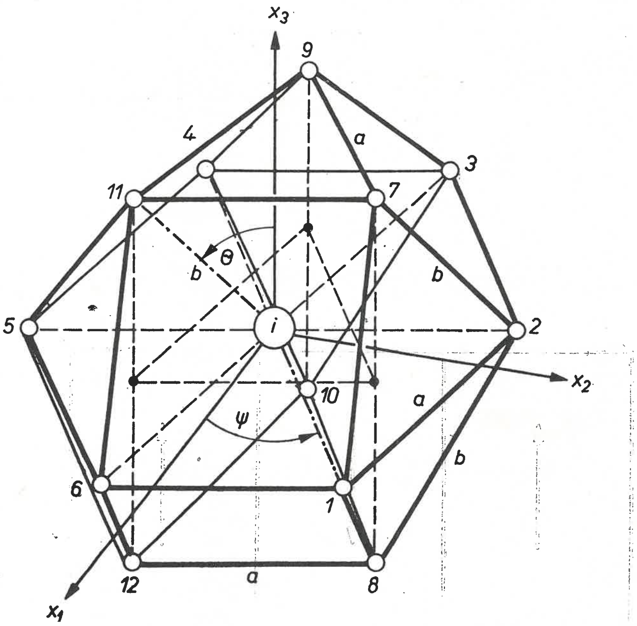

Fig. 1. Labelling of the atoms in the first coordination sphere of the close-packed hexagonal crystal lattice

In labelling the sites within the first coordination sphere of the hexagonal close-packed lattice (Fig. 1) we use a similar notation as in [8]. Thus, the components of the nearest-neighbour lattice vectors can be written in the form

$$(r_{ij}^a) = a \begin{pmatrix} \cos[\psi+\pi(j-1)/3] \\ \sin[\psi+\pi(j-1)/3] \\ 0 \end{pmatrix} \tag{3}$$

for $j \leqslant 6$, and

$$(r_{ij}^a) = b \begin{pmatrix} \gamma\cos[\psi+\pi/6+2\pi(j-1)/3] \\ \gamma\sin[\psi+\pi/6+2\pi(j-1)/3] \\ (-1)^{j+1}(1-\gamma^2)^{1/2} \end{pmatrix} \tag{4}$$

for $6 < j \leqslant 12$ where $\gamma = \sin\theta = a/b\sqrt{3}$, the angle ψ is arbitrary, and the coefficients a and b denote the nearest-neighbour distances between atoms belonging to the same and to neighbouring hexagonal crystal planes, respectively. (They are not to be confused with the tensor indices).

We choose the hexagonal crystal axis as the x_3-axis of our coordinate system (direction of easiest magnetization) and assume the 180° Bloch walls to lie in the $x_2 0 x_3$ plane, as shown schematically in Fig. 2 for the field-free case. (Note that, according to [8], the hexagonal axis [0001] is magnetically preferred if $b < a$). Hence, upon specifying

$$\mathscr{H}^a = \mathscr{H}\delta^{a1}$$

we have a transversal magnetic field of strength $\mathscr{H}$ which is perpendicular to the Bloch walls. The magnetostatic self-energy of the sample in its own demagnetizing field (originating from the magnetic poles on the basal crystal surfaces) is neglected in the Hamiltonian (1).

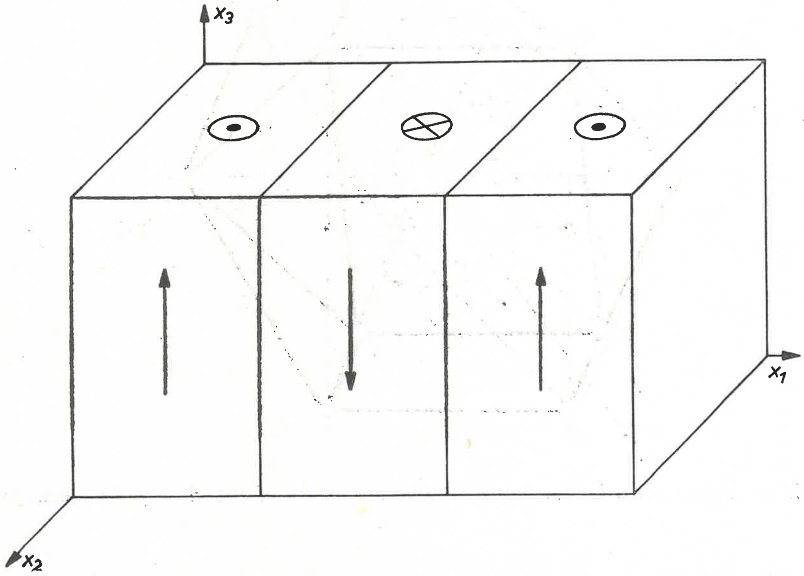

Fig. 2. Model of the plate-like Kittel-type domain structure

In the familar one-dimensional model of the Kittel-type domain structure, the atomic magnetic moments all lie in the $x_2 0 x_3$ plane and vary merely their direction on passing from one domain to another. Thus, in the field-free case their direction can be described by the angle φ measured, *e. g.*, from the x_3-axis (Fig. 3) and depending only on the variable x_1. For simplicity, we assume that the field (5) inclines all the magnetic moments uniformly toward the field direction, *i. e.*, the inclination can be described by a single angle ϑ measured from the field direction and depending only on the field strength $\mathscr{H}$, Fig. 3. Thus, the problem reduces to determining the functions $\varphi(x_1)$ and $\vartheta(\mathscr{H})$.

Let us define the unitary transformations U and V,

$$U = \prod_i U_i, \quad U_i = \exp(i\varphi_i S_i^1), \quad US_i^a U^+ = U_i S_i^a U_i^+ = U_i^{ab} S_i^b,$$

$$(U_i^{ab}) = \begin{pmatrix} 1 & 0 & 0 \\ 0 & \cos\varphi_i & -\sin\varphi_i \\ 0 & \sin\varphi_i & \cos\varphi_i \end{pmatrix}, \tag{6}$$

$$V = \prod_i V_i, \quad V_i = \exp(i\vartheta S_i^2), \quad VS_i^a V^+ = V_i S_i^a V_i^+ = V^{ab} S_i^b,$$

$$(V^{ab}) = \begin{pmatrix} \cos\vartheta & 0 & \sin\vartheta \\ 0 & 1 & 0 \\ -\sin\vartheta & 0 & \cos\vartheta \end{pmatrix}, \tag{7}$$

of which the first one corresponds to an inhomogeneous rotation of the lattice spins about the x_1-axis by the angles φ_i, while the second one rotates the spins uniformly about the x_2-axis by the angle ϑ. Now, according to [6–8] the equilibrium domain structure

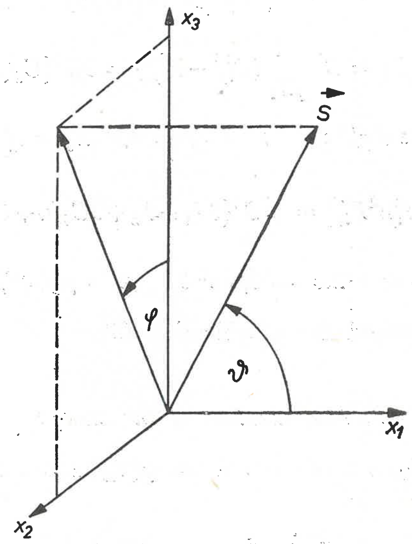

Fig. 3. Definition of rotation angles φ and ϑ

should correspond to the minimum (with respect to $\varphi(x_1)$ and $\vartheta(\mathscr{H})$) of the following mean energy:

$$\tilde{h}(\varphi_i, \vartheta) = \langle \varphi_i, \vartheta | H | \varphi_i, \vartheta \rangle = \langle 0 | WHW^+ | 0 \rangle =$$

$$= -\mu g S \sum_i \mathscr{H}^a W^{a3} - \tfrac{1}{2} S^2 \sum_{ij} P_{ij}^{ab} W_i^{a3} W_j^{b3} \tag{8}$$

where $W = UV$, $W_i^{ab} = U_i^{ac} V^{cb}$, S is the maximum spin eigenvalue, and $|0\rangle$ is the saturation state in which all the spins are aligned along the positive x_3-axis.

The next step resides in passing to continuous variables,

$$\{\varphi_i\} \to \varphi(x_1), \quad \sum_i \to V_0^{-1} \int_{\tilde{V}} dv \tag{9}$$

where $V_0 = \tilde{V}/N = a^3(1-\gamma^2)^{1/2}/2\gamma$, $\tilde{V}$ being the volume of the crystal (assumed to be a rectangular prism with dimensions L_1, L_2, L_3 in the directions x_1, x_2, x_3, respectively) and N the number of lattice atoms. With the approximations made in [8] we finally obtain for the mean energy $h = \tilde{h}/\tilde{V}$ per unit volume the formula

$$h = Q_0 + Q_1 \sin^2\vartheta \int_0^{L_1} \{\kappa^{-2}\dot{\varphi}^2 - \cos^2\varphi + V(\vartheta)\}dx_1 \tag{10}$$

where

$$Q_0 = 2S^2V_0^{-1} \sum_{j=1}^{12} P_{ij}^{11} = 2S^2V_0^{-1}\{6(J_1+J_2)-3C_1-3C_2(3\gamma^2-2)\},$$

$$J_{ij}, C_{ij} = \begin{cases} J_1, C_1 \text{ for } j \leqslant 6, \\ J_2, C_2 \text{ for } 6 < j \leqslant 12, \end{cases} \tag{11}$$

$$Q_1 = \eta/V_0L_1, \quad 2\eta = S^2 \sum_{j=1}^{12} (P_{ij}^{11} - P_{ij}^{33}) = 9S^2\{C_2(2-3\gamma^2)-C_1\},$$

$$\dot{\varphi} \equiv d\varphi/dx_1, \quad \kappa = \kappa_0 \sin\vartheta, \quad \kappa_0^2 = \eta/\varrho,$$

$$4\varrho = S^2 \sum_{j=1}^{12} (r_{ij}^1)^2 P_{ij}^{22} = a^2S^2\{3J_1+J_2+3C_1/4+C_2(1-3\gamma^2/4)\},$$

$$V(\vartheta) = -2\omega \cos\vartheta/\sin^2\vartheta, \quad \omega = \mu g S\mathscr{H}/2\eta.$$

In deriving Eq. (10) we utilized the specification (5).

3. *Minimization of the energy*

The energy density (10) is a functional on $\varphi(x_1)$ and a function of ϑ. The Euler--Lagrange equation

$$\kappa^{-2}\ddot{\varphi} - \sin\varphi \cos\varphi = 0 \tag{12}$$

is actually the same as for the field-free case in [8]. The first integration leads to

$$\kappa^{-2}\dot{\varphi}^2 = C - \cos^2\varphi \tag{13}$$

and the constant C can be determined from the periodicity condition

$$\varphi(x_1 \pm n\Delta) = \varphi(x_1) \pm n\pi, \quad n = 0, 1, 2, \ldots \tag{14}$$

which upon the second integration takes the form

$$\int_0^{2\pi} \frac{d\varphi}{\kappa\sqrt{C-\cos^2\varphi}} = 2\Delta \tag{15}$$

where Δ is the domain width. According to experimental investigations [16], Δ can be assumed as being field-independent. The condition (15) relates Δ (which is to be considered as external parameter) to the modulus $k^2 = C^{-1}$ of the complete elliptic integral $\boldsymbol{K}(k)$ of the first kind,

$$\boldsymbol{K}(k) = \kappa\Delta/2k = \kappa_0\Delta \sin\vartheta/2k, \tag{16}$$

which, in turn, determines the solution of Eq. (13),

$$\cos\varphi = -\mathrm{sn}(qx_1), \quad q = \kappa_0 k^{-1}\sin\vartheta. \tag{17}$$

The above solution depends on the field strength $\mathscr{H}$, through ϑ. To determine this dependence, let us assume $L_1/2\Delta = m$, where m is a positive integer, and calculate the energy (10) for the solution (17). By utilizing Eqs (13), (14) we obtain

$$h = Q_0+2Q_1 k\kappa^{-1}\sin^2\vartheta \int_0^{2\pi}\left\{\frac{p-\sin^2\psi}{\sqrt{1-k^2\sin^2\psi}}\right\}d\psi, \tag{18}$$

$$p = \tfrac{1}{2}[V(\vartheta)+k^{-2}]$$

which, by making use of the relation (16), leads to the result

$$h = Q_0+8Q_1\{E\kappa_0^{-1}k^{-1}\sin\vartheta-\Delta[2\omega k^2\cos\vartheta+\sin^2\vartheta]/4k^2\} \tag{19}$$

where $\boldsymbol{E} = \boldsymbol{E}(k)$ is the complete elliptic integral of the second kind. In minimizing Eq. (19) with respect to ϑ we note that

$$dh/d\vartheta = \partial h/\partial\vartheta+[(\partial h/\partial \boldsymbol{E})(d\boldsymbol{E}/dk)+\partial h/\partial k](dk/d\vartheta). \tag{20}$$

However, one easily verifies that in our case the sum in the brackets vanishes, due to Eqs (16), (19) and the relation (cp. [28])

$$d\boldsymbol{E}/dk = (\boldsymbol{E}-\boldsymbol{K})/k. \tag{21}$$

Hence, the necessary minimum condition reduces to $\partial h/\partial\vartheta = 0$ which leads to the equation

$$2k\boldsymbol{E}\kappa_0^{-1}\Delta^{-1}\cos\vartheta-\sin\vartheta\cos\vartheta+\omega k^2\sin\vartheta = 0. \tag{22}$$

The solution of this equation that corresponds to a minimum of h is

$$\tan\vartheta = 2(\boldsymbol{K}-\boldsymbol{E})/\omega k\kappa_0\Delta = -2(d\boldsymbol{E}/dk)/\kappa_0\omega\Delta. \tag{23}$$

For the field-free case $\omega = \mathscr{H} = 0$, $\vartheta = \pi/2$ we conclude from Eq. (16) and [8] that $0 < k < 1$ (for finite Δ), hence $d\boldsymbol{E}/dk \neq 0$, while for $\omega\sim\mathscr{H}\to\infty$ Eqs (16) and (23) imply that $k\to 0$, in which case $(d\boldsymbol{E}/dk)\to 0$ (cp. [29]). Thus, the solution (23) has the physically correct limit values

$$\lim_{\omega\to 0}\vartheta = \lim_{\mathscr{H}\to 0}\vartheta = \pi/2, \quad \lim_{\omega\to\infty}\vartheta = \lim_{\mathscr{H}\to\infty}\vartheta = 0 \tag{24}$$

and is a continuous and monotonic function od the field strength $\mathscr{H}$, as $\boldsymbol{K}$, $\boldsymbol{E}$ and $d\boldsymbol{E}/dk$ are continuous and monotonic functions of the modulus k.

4. The magnetization curve

If $L_1/2\Delta$ is an integer, the net longitudinal magnetization (*i.e.*, the magnetization component along the anisotropy axis x_3) of the sample is obviously zero, like in the field-free case. Let us thus calculate the transversal magnetization along the field-direction, which is given by the simple formula (per unit volume)

$$I(\omega) = I_0 \cos \vartheta = I_0 \cos \arctan\,[2(K-E)/\omega k \kappa_0 \Delta] \qquad (25)$$

where $I_0 = \mu g S/V_0$ is the saturation magnetization per unit volume. From Eq. (24) it follows that

$$\lim_{\omega\to 0} I = \lim_{\mathscr{H}\to 0} I = 0, \quad \lim_{\omega\to\infty} I = \lim_{\mathscr{H}\to\infty} I = I_0, \qquad (26)$$

and that I is a continuous and monotonic function of the field strength $\mathscr{H}$.

5. *The magnetic susceptibility*

The transversal magnetic susceptibility $\chi = dI/d\mathscr{H}$ is conveniently expressed through the relative magnetization $I^* = I/I_0$ and the relative susceptibility χ^* as follows:

$$\chi(\mathscr{H}) = I_0(dI^*/d\omega)(d\omega/d\mathscr{H}) \equiv I_0((d\omega/d\mathscr{H})\chi^* = (\mu g S I_0/\eta)\chi^*(\omega). \qquad (27)$$

Hence, from Eq. (25) we obtain

$$\chi^*(\omega) = \{2\kappa_0 \Delta k(K-E)/[(\omega\Delta k\kappa_0)^2+16(K-E)^2]-$$
$$-2(k^2K-E)(dk/d\omega)/\omega\kappa_0 k^2 k_0^2 \Delta\} \sin \arctan\,[2(K-E)/\omega\kappa_0 k\Delta] \qquad (28)$$

where $k^2{}_0 = 1-k^2$. By utilizing Eqs (16), (23), (24) and the behaviour of the complete elliptic integrals $K(k)$, $E(k)$ for $k \to 0$ and $k \lesssim 1$ (cp. [29]), one easily proves that

$$\lim_{\omega\to 0} \chi^* = (\eta/\mu g S I_0) \lim_{\mathscr{H}\to 0} \chi = 1, \quad \lim_{\omega\to\infty} \chi^* = \lim_{\mathscr{H}\to\infty} \chi = 0, \qquad (29)$$

and that χ is a continuous and monotonic function of the magnetic field strength $\mathscr{H}$.

6. *The Bloch wall thickness*

The thickness δ of the 180° Bloch wall can be defined as (cp. [2–5])

$$\delta = \pi/|\dot{\phi}(\varphi = \pi/2)|. \qquad (30)$$

This definition is illustrated in Fig. 4 for the solution (17) in the case $k \lesssim 1$, *i.e.*, $\kappa\Delta \gg 1$ (weak field and large domain width, *i.e.*, large crystal thickness L_3; cp. [30–33]). Noting that $C^{-1} = k^2$, Eq. (13) leads for $\varphi = \pi/2$ to the result

$$\delta = \pi k/\kappa_0 \sin \vartheta \equiv \delta_0 k/\sin \vartheta. \qquad (31)$$

From Eqs (16), (24) we easily conclude that $\mathscr{H} \to \infty$ implies $k \to 0$, in which case $K \to \pi/2$ (cp. [28, 29]). Thus, we obtain the physically reasonable limit values

$$\lim_{\mathscr{H}\to 0} \delta = \delta_0 k, \quad \lim_{\mathscr{H}\to\infty} \delta = \Delta, \qquad (32)$$

of which the first one coincides with the field-free result obtained in [8]. As in this case $k \to 1$ for $\Delta \to \infty$, Eq. (16), we see that $\delta_0 k \to \delta_0$ in the asymptotic limit of the phenomenological theory [10, 34, 35]. Like the magnetization and susceptibility, the Bloch wall thickness (31), too, is a continuous and monotonic function of the external field strength $\mathscr{H}$.

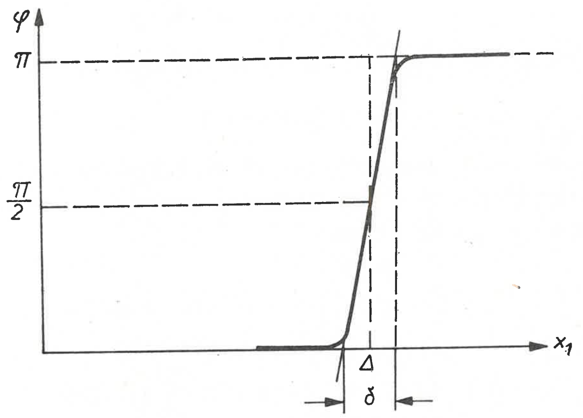

Fig. 4. Definition of the Bloch wall thickness δ

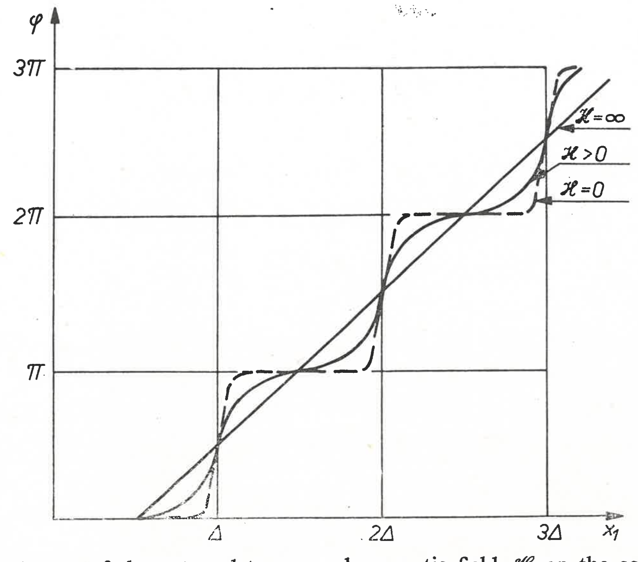

Fig. 5. Influence of the external transversal magnetic field $\mathscr{H}$ on the solution (17)

From Eqs (16) and (23) it follows that for very large field strengths $k \to 0$, *i.e.*, $\boldsymbol{K} \to \pi/2$, in which case the solution (17) approaches the asymptotic form [29]

$$\cos\varphi \cong -\sin qx_1, \quad i.e., \quad \varphi \cong qx_1 - \pi/2 \tag{33}$$

with $q \to 2K/\Delta \to \pi/\Delta$. Thus, with increasing field strength the angle φ becomes gradually a linear function of x_1, the walls becoming hardly distinguishable from domains (spiral structure), as shown schematically in Fig. 5. At the same time, however, the spin spiral folds down upon the field direction, as $\vartheta \to 0$ (cp. Fig. 3).

7. *The Bloch wall energy*

According to [8], we can define the energy density σ per unit area of the Bloch wall as

$$\sigma = \Delta(h-h_0) \tag{34}$$

where h and h_0 denote respectively the value of the functional (10) for the solution (17) and for the saturation state $\dot{\varphi} = \varphi = 0$. Denoting $qx_1 = t$ and making use of Eqs (13), (16), (17), (23) and $C^{-1} = k^2$ we obtain

$$\begin{aligned} \sigma &= Q_1 L_1 \sin^2 \vartheta \int_0^{\Delta} (1+C-2\cos^2 \varphi) dx_1 = \\ &= Q_1 L_1 \Delta K^{-1} \sin^2 \vartheta \{k_0^2 K/k^2 + \int_{-K}^{K} \mathrm{cn}^2 t dt\} = \\ &= 2Q_1 L_1 k^{-1} \kappa_0^{-1} (2E - k_0^2 K) \sin \vartheta = \\ &= 2\eta V_0^{-1} k^{-1} \kappa_0^{-1} (2E - k_0^2 K) \sin \arctan [2(K-E)/k\kappa_0 \omega \Delta] \end{aligned} \tag{35}$$

when noting that

$$\int_0^{L_1} dx_1 = (L_1/\Delta) \int_0^{\Delta} dx_1 \tag{36}$$

due to Eq. (14). From Eqs (16, (21) and (24) we get, similarly as in Eq. (28), the limit values

$$\begin{aligned} \lim_{\mathscr{H}\to 0} \sigma &= 2\eta(2E-k_0^2K)/kV_0\kappa_0 \equiv \sigma_0(2E-k_0^2K)/2k, \\ \lim_{\mathscr{H}\to \infty} \sigma &= 0 \end{aligned} \tag{37}$$

and readily prove that σ, like all foregoing quantities, is a continuous and monotonic function of the field strength $\mathscr{H}$. As $k \to 1$ for $\Delta \to \infty$ and weak fields, cp. Eq. (16), we have in this case the asymptotic field-free limit $\sigma \to \sigma_0$, in agreement with phenomenological results [34, 35]. On the other hand, the field-free limit in (37) agrees with the result obtained in [8] in the field-free case.

Let us note that the formula (35) can be simplified if $\kappa\Delta \gg 1$ (small field and large domain width, *i.e.*, large crystal thickness L_3; cp. [30–33]), as in this case Eq. (16) implies $k \lesssim 1$. This permits to use in (35) the asymptotic formula (cp. [29])

$$\mathrm{cn}\, t \cong \mathrm{sech}\, t \tag{38}$$

which leads to the simpler expression

$$\sigma \cong 2Q_1 L_1 \kappa_0^{-1} \tanh(\kappa_0 \Delta \sin \vartheta) \sin \vartheta. \tag{39}$$

8. *Numerical calculations and comparison with experiment*

As the only experimental data which can be reasonably compared with our results are the magnetization curves measured for single-crystalline Co in [17], we confine ourselves in the present paper to examining numerically the formula (25) for the magnetization and defer the numerical analysis of the remaining quantities to a separate paper [36]. We shall compare our numerical magnetization curve with that obtained in [17] for the layer-like (and complex, cp. [32]) Goodenough-type domain structure in the case when the transversal magnetizing field was perpendicular to the domain layers (*i.e.*, parallel to the "creating" field H_E used in producing the structure; cp. [16]). Actually, two such cases have been examined in [17], in which the magnetizing (and the creating) field was parallel either to the crytallographic direction $[01\bar{1}0]$ or $[2\bar{1}\bar{1}0]$ (Figs 3a and 6a in [17], respectively). Our calculations do not take into account the slight anisotropy of the hexagonal lattice within the basal crystal plane (0001) (cp. [8]) but, fortunately, the respective magnetization curves in [17] do not differ significantly either, although there are subtle differences in the corresponding domain structures (*cp.* [16, 32]).

It should be noted, however, that, even for small field strengths, the above mentioned experimental magnetization curves cannot be expected to agree quantitatively with our theoretical results. For one thing the initial magnetization curves in [17] have been found to depend on the sign of the magnetizing field (reversal of field direction), a rather perplexing (and apparently substructural) effect which is neither experimentally nor theoretically explained, except that it must be attributable to the specific process in which those (remanent) domain structures are obtained. On the other hand, the 180° Bloch walls of the complex Goodenough structure studied in [17] are extremely wavy at the basal crystal surfaces and, in addition, there is a highly complicated array of spike-like closure domains at these crystal surfaces (cp. [37]). Neither of these modifications is included in our simple domain structure model, as either one is mathematically hard to handle even in the phenomenological approach (*cp.* [31]). Finally, a rather important factor in aiming at quantitative agreement with experimental data is the sample's demagnetizing energy (cp. [31, 35]) which has been neglected in our theory. In view of these shortcomings of the present theory it is a pity that the measurements of [17] have not yet been repeated on thin Co single crystals ($L_3 < 50$ μm), as in this case the complex Goodenough domain structure is known to pass gradually into the simple plate-like Kittel-type structure assumed in this paper (*cp.* [31, 32]). None the less, it appears that our results are at least for small field strengths in qualitative agreement with the corresponding experimental curves given in [17].

In carrying out the numerical calculations, we shall express the microscopic constants involved in Eq. (25) through the more accurate macroscopic constants A (exchange constant), K_1 (first anisotropy constant) and I_0 which, according to [35], have for Co the following values (at room temperature):

$$A = 1.3 \cdot 10^{-6}\ \text{erg/cm},\quad K_1 = 4.3 \cdot 10^{6}\ \text{erg/cm}^3,\quad I_0 = 1422\ \text{Gs}. \tag{40}$$

The relationship between these constants can be established quite easily, by comparing Eq. (10) with the respective functional for uniaxial ferromagnets following from the phenomenological theory (cp. [2, 3, 35]). It reads

$$\varrho = AV_0,\ \eta = K_1 V_0,\ \kappa_0^2 = \eta/\varrho = K_1/A,$$

$$\omega = I_0 V_0 \mathscr{H}/2\eta = I_0 \mathscr{H}/2K_1 \tag{31}$$

and leads with the values (40) to

$$\kappa_0 = 1.8\cdot 10^6\ \mathrm{cm}^{-1},\ \omega = 1.7\cdot 10^{-4}\mathscr{H}\ \mathrm{Gs\ cm^3/erg}. \tag{42}$$

For the domain width we take the value $\Delta = 10^{-2}$ cm from [17], in which case $\kappa_0\Delta > 10^4$ and, according to a numerical analysis of Eqs (16) and (23), the modulus k is over a wide field range very close to 1 as, *e.g.*, $k_0^2 = 1-k^2 < 10^{-9}$ for fields up to 6000 Oe. This permits to use the expansion [28, 29]

$$\boldsymbol{K}(k) = \ln(4k_0^{-1}) + (1/2)^2 \ln(4k_0^{-1}-1) + \ldots \tag{43}$$

for the complete elliptic integral of the first kind, which considerably simplifies the calculations.

The result of our numerical analysis, based on Eqs (16), (23), and (25), is shown in Figs 6 and 7 (bold curves). In Fig. 6 the dashed curves represent experimental results (cp. Fig. 3a in [17]). It is seen that the theoretical curve agrees qualitatively only with the

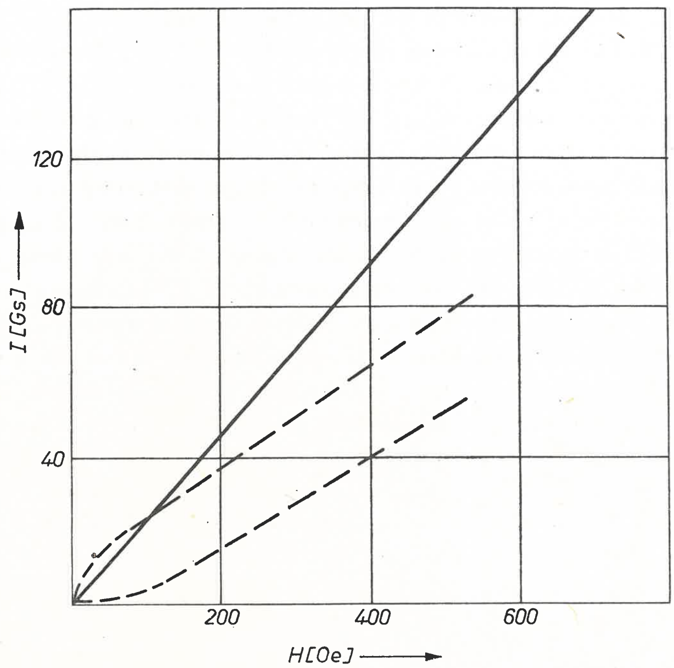

Fig. 6. Comparison of the weak-field theoretical magnetization curve (bold line) with the experimental curves (dashed lines) obtained for Co in [17] (Fig. 3a)

upper experimental curve (opposite directions of the magnetizing and creating field), and even then only in the weak-field region (up to 200 Oe). It is rather obvious that the main reason of this poor agreement is, above all, the neglect of the sample's demagnetizing field in our considerations, as this field actually lessens the strength of the external field inside the sample and thus impedes substantially the magnetization process.

As regards the field-induced ferro-paramagnetic phase transition shown to exist in uniaxial single-domain ferromagnets in a transversal magnetic field [19–26], it is seen to be cancelled by the domain structure, as the susceptibility (28) is a continuous function

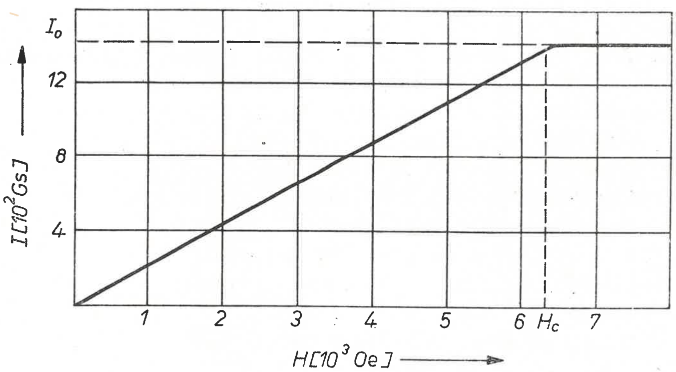

Fig. 7. Theoretical magnetization curve (25) for Co. (Note the "ferro-paramagnetic" pseudo-phase transition at the pseudo-critical field strength $\mathscr{H}_c$)

of the field strength. The only trace of it is the "pseudo-phase-transition" clearly visible in Fig. 7 and taking place at the "pseudo-critical field" strength $\mathscr{H}_c$ of about 6200 Oe, at which the magnetization attains practically saturation. Note that $I_0\mathscr{H}_c \approx 2K_1 = 8.6 \cdot 10^6$ erg/cm^3 for Co, *i.e.*, $\mathscr{H}_c$ corresponds to $\omega \approx 1$. Bellow this field strength the susceptibility is practically constant, while above it it is effectively zero, *i.e.*, like in the limit cases (29). It is very unlikely that the inclusion of the demagnetizing energy into the theory will alter this result — except for shifting upwards the pseudo-critical field strength and perhaps smearing out the pseudo-phase-transition itself. This conclusion is corroborated by experimental investigations (cp. [27, 35, 38]) in which, unfortunately, little attention has been paid to the domain structure itself.

There is, however, a chance that the phase transition does exist even in the presence of the domain structure if the transversal magnetic field is parallel to the Bloch walls, as in this case the Euler-Lagrange equation has two different periodic solutions confined to two non-overlapping field intervals [3, 5]. The solutions are continuous at the dividing point, but the magnetization and susceptibility have not yet been studied and the latter may well be discontinuous. Such investigations are under way and the results shall be published in a subsequent paper [39]. The so-called threshold fields arrived at in [14] while examining this case in the molecular-field approximation might also indicate the existence of a phase transition.

Finally, it should be emphasized that the magnetization (25) (as well as the remaining quantities (28), (31) and (35)) depends on the domain width Δ, *i.e.*, on the crystal thickness L_3 in the magnetically preferred direction [0001] (cp. [31–33]). The numerical analysis of this dependence will be carried through in a separate paper [39]. However, it would be very interesting to study this problem also experimentally, by extending the measurements of [17] to the series of single-crystalline Co samples examined in [32]. It is quite possible that Δ (*i.e.*, L_3) may affect the value of $\mathcal{H}_c$ and hence the slope of the magnetization curve below $\mathcal{H}_c$.

REFERENCES

[1] C. Kittel, *Rev. Mod. Phys.*, **21**, 541 (1949); C. Kittel, J. Galt, *Solid State Phys.*, **3**, 437 (1956).
[2] M. J. Shirobokov *Zh. Eksper. Teor. Fiz.*, **15**, 57 (1945).
[3] M. J. Shirobokov, *Dokl. Akad. Nauk. SSSR*, **24**, 426 (1939).
[4] W. J. Ziętek, *Acta Phys. Polon., Suppl*, **22**, 127 (1962).
[5] W. J. Ziętek, *Acta Phys. Polon.*, **23**, 363 (1963).
[6] W. J. Ziętek, *Acta Phys. Polon.*, **21**, 175 (1962).
[7] W. J. Ziętek, *Phys. Status Solidi*, **8**, 65 (1965).
[8] J. Klamut, W. J. Ziętek, *Proc. Phys. Soc.*, **82**, 264 (1963).
[9] J. Klamut, *Acta Phys. Polon.*, **25**, 711 (1964); **30**, 65 (1966).
[10] W. Wasilewski, *Acta Phys. Polon.*, **30**, 577 (1966).
[11] H. Pfeiffer, J. Ulner, *Acta Phys. Polon.*, **A39**, 703 (1971).
[12] J. Klamut, *Acta Phys. Polon.*, **31**, 555 (1967).
[13] J. Klamut, W. Wasilewski, *Acta Phys. Polon.*, **33**, 147 (1968).
[14] J. Klamut, *Acta Phys. Polon.*, **A38**, 873, (1970); **A39**, 273 (1971).
[15] J. Kowalski, *Acta Phys. Polon.*, **32**, 309 (1967).
[16] B. Wysłocki, *Acta Phys. Polon.*, **27**, 783, 955 (1965).
[17] B. Wysłocki, *Acta Phys. Polon.*, **27**, 969 (1965).
[18] A. Wachniewski, *Acta Phys. Polon.*, **33**, 923 (1968).
[19] P. Wojtowicz, M. Rayl, *Phys. Rev. Letters*, **20**, 1489 (1968).
[20] E. Riedel, F. Wegner, *Z. Phys.*, **225**, 195 (1969).
[21] H. Thomas, *Phys. Rev.*, **187**, 630 (1969).
[22] K. Durczewski, *Acta Phys. Polon.*, **A38**, 855 (1970).
[23] J. Sznajd, *Phys. Status Solidi*, **41**, 405 (1970).
[24] H. Pfeiffer, *Acta Phys. Polon.*, **A39**, 213 (1971).
[25] G. Kozłowski, L. Biegała, S. Krzemiński, *Acta Phys. Polon.*, **A39**, 417 (1971).
[26] J. Ulner, *Acta Phys. Polon.*, **A40**, 725 (1971).
[27] H. Suzuki, T. Watanabe, *J. Phys. Soc. Japan*, **30**, 367 (1971).
[28] F. Oberhettinger, W. Magnus, *Anwendung der elliptischen Funktion in Physik und Technik*, Springer-Verlag, Berlin—Heidelberg—New York 1949.
[29] I. S. Gradshtayn, I. M. Ryzhik, *Tables of integrals, sums, series and products*, 5-th edition, Science Publ. House, Moscow 1971 (in Russian).
[30] J. Ulner, W. J. Ziętek, *Acta Phys. Polon.*, **35**, 127 (1969); K. Durczewski, W. J. Ziętek, *Acta Phys. Polon.*, **35**, 307 (1969).
[31] G. Kozłowski, W. J. Ziętek, *Acta Phys. Polon.*, **29**, 261, (1966); **A42**, 87 (1972).
[32] B. Wysłocki, *Acta Phys. Polon.*, **34**, 327 (1968); **35**, 179 (1969); B. Wysłocki, W. J. Ziętek, *Phys. Letters*, **29A**, 114 (1969).
[33] S. Szymura, B. Wysłocki, W. J. Ziętek, *Acta Phys. Polon.*, **A38**, 405 (1970).
[34] B. A. Lilley, *Phil. Mag.*, **41**, 792 (1950).

[35] A. Seeger (editor), *Chemische Bindung in Kristallen und Ferromagnetismus*, Springer-Verlag, Berlin—New York 1966.
[36] W. Wasilewski, *Acta Phys. Polon.*, **A42** (1972) — in the press.
[37] B. Wysłocki, *Phys. Status Solidi*, **3**, 1333 (1963); *Ann. Phys.* (Germany), **13**, 109 (1964); B. Wysłocki, W. J. Ziętek, *Acta Phys. Polon.*, **29**, 223 (1966).
[38] S. Kaya, *Sci. Rep. Tohoku Univ.*, **17**, 639, 1157, 1165 (1928); C. Guillaud, *J. Phys. Radium*, **12**, 492 (1951); W. Sucksmith, J. E. Thompson, *Proc. Roy. Soc.*, **A225**, 362 (1954).
[39] W. Wasilewski, W. J. Ziętek — to be published.